UvA-DARE (Digital Academic Repository)

Multipodal coordination of a tetracarboxylic crown ether with NH4+: a vibrational spectroscopy and computational study

Hurtado, P.; Gámez, F.; Hamad, S.; Martínez-Haya, B.; Steill, J.D.; Oomens, J.

Link to publication

Multipodal coordination of a tetracarboxylic crown ether with NH 4+: A vibrational spectroscopy and computational study

Paola Hurtado, Francisco Gámez, Said Hamad, Bruno Martínez–Haya, Jeffrey D. Steill et al.

Additional information on J. Chem. Phys.

Multipodal coordination of a tetracarboxylic crown ether with NH_4^+: A vibrational spectroscopy and computational study

Paola Hurtado,[1] Francisco Gámez,[1] Said Hamad,[1] Bruno Martínez–Haya,[1,a)]
Jeffrey D. Steill,[2] and Jos Oomens[3]

[1]*Department of Physical, Chemical and Natural Systems, Universidad Pablo de Olavide, 41013 Seville, Spain*
[2]*FOM Institute for Plasma Physics Rijnhuizen, Edisonbaan 14, NL-3439 MN Nieuwegein, The Netherlands*
[3]*University of Amsterdam, Science Park 904, 1098XH Amsterdam, The Netherlands*

The elucidation of the structural requirements for molecular recognition by the crown ether (18–crown–6)-2,3,11,12-tetracarboxylic acid (18c6H4) and its cationic complexes constitutes a topic of current fundamental and practical interest in catalysis and analytical sciences. The flexibility of the central ether ring and its four carboxyl side arms poses important challenges to experimental and theoretical approaches. In this study, infrared action vibrational spectroscopy and quantum mechanical computations are employed to characterize the conformational structure of the isolated gas phase complex formed by the 18c6H4 host with NH_4^+ as guest. The results show that the most stable gas–phase structure is a barrel–like conformation sustained by tetrapodal H–bonding of the ammonia cation with two C=O side groups and with four oxygen atoms of the ether ring in a bifurcated arrangement. Interestingly, a similar structure had been proposed in previous crystallographic studies. The experiment also provides evidence for a significant contribution of a higher energy bowl–like conformer with features resembling those adopted by 18c6H4 in the analogous complexes with secondary amines. Such a conformation displays H−bonding between confronted side carboxyl groups and tetrapodal binding of the NH_4^+ with the ether ring and with one C=O group. Structures involving even more extensive intramolecular H–bonding in the 18c6H4 substrate are found to lie higher in energy and are ruled out by the experiment. © *2012 American Institute of Physics.* [http://dx.doi.org/10.1063/1.3693518]

I. INTRODUCTION

Molecular recognition by substrates based on substituted crown ethers constitutes an active field of research that is strongly stimulated by technological applications in catalysis and separation sciences.[1–9] This study focuses on the conformational behavior of one of the most common substrates of this kind, namely, (18–crown–6)-2,3,11,12-tetracarboxylic acid (henceforth, 18c6H4), upon complexation with ammonium (NH_4^+). The 18c6H4–NH_4^+ system is of fundamental interest on its own and as a model for the multipodal coordination arrangements that characterize the complexes formed by the 18c6H4 host.

Previous studies with x–ray crystallography and nuclear magnetic resonance spectroscopy have demonstrated the affinity of 18c6H4 for protonated amines, amino acids, amino alcohols and further compounds with free amino functionality.[8–16] Those studies have provided evidence for the relevance of the barrel–like and bowl–like structures adopted by 18c6H4. Such structures are sustained by intramolecular H–bonding involving the carboxyl groups and by intermolecular interactions of the cationic guest with the ether and carboxyl oxygen atoms. Binding selectivity is in addition modulated by steric repulsion between the side chains of the guest (e.g., a primary amine) and the substrate. Since the 18c6H4 molecule is chiral, particular efforts have been devoted in those studies to enantiomeric discrimination in the amine complexes. The (+)-18c6H4 enantiomer is represented in Fig. 1, which illustrates that chirality is related to the spatial orientation of its four carboxyl pending arms.

The present work shows that the barrel and bowl conformations typically adopted by 18c6H4 can be investigated in the gas phase by means of laser spectroscopic and mass spectrometric techniques. The potential of current gas–phase techniques has motivated a surge of investigations on relatively complex organic and biomolecular systems that has been reviewed in a textbook[17] and in several comprehensive surveys.[18–21] In this study, electrospray ionization and Fourier-transform ion cyclotron resonance mass spectrometry (ESI–FT–ICR) are employed to produce, mass–select, and store the 18c6H4–NH_4^+ complex at room temperature. Infrared multiple photon dissociation (IRMPD) action spectroscopy is then applied to characterize its vibrational modes. The experiment covers the fingerprint mid–infrared region (500–2000 cm^{-1}), with the C–C, C–O, and C=O stretching bands and the CH2 and NH4 deformation bands as references. A general description and technical details of the experimental procedure and of the complementary computational methods are provided in Sec. II.

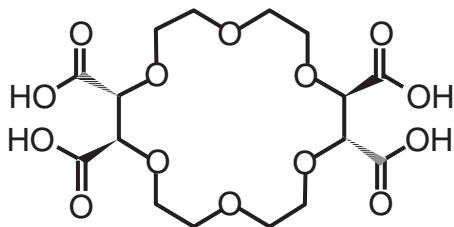a)Author to whom correspondence should be addressed. Electronic mail: bmarhay@upo.es.

136, 114301-1

FIG. 1. Schematic representation of the molecule (+)-(18-crown-6)-2,3,11,12-tetracarboxylic acid (referred to as $18c6H_4$ throughout the paper).

II. METHODS

A. ESI-FTICR IRMPD spectroscopy

Infrared multiple photon dissociation spectra were recorded using a FT–ICR mass spectrometer, coupled to the beamline of the free electron laser FELIX.[22] The $18c6H_4$–NH_4^+ complex was produced via electrospray of 1 mM solutions of the crown ether and NH_3 in a water/methanol mixture with added acetic acid. Ions are accumulated in a hexapole ion trap and then pulse injected into the ICR cell, where they are mass isolated. The mass-selected ions are then irradiated with typically 10 FELIX macro–pulses. Each macro–pulse is approximately 5 μs long, has an energy of about 35 mJ, and consists of a train of micro–pulses with a repetition frequency of 1 GHz. The nominal spectral bandwidth of the radiation amounts to 0.5% of the central wavelength. Further description of typical experimental procedures can be found in Ref. [23].

If the infrared wavelength is in resonance with a vibrational mode of the complex, multiple photon absorption occurs leading to dissociation of the parent ion. The IRMPD spectrum is constructed by plotting the relative ionic fragment yield as a function of the wavenumber of the radiation. The main IRMPD fragments observed for $18c6H_4$–NH_4^+ corresponded to the loss of ammonia, hence yielding protonated $18c6H_4$ (m/z=441), and to the cleavage of one or two of the carboxyl arms with the eventual additional loss of one water molecule (m/z=395, 377, 349, and 331). The recorded spectra were linearly corrected for the changes in laser pulse power, in consonance with the linear laser power dependence of the non-coherent multiple photon dissociation yield characteristic of IRMPD.[20] The intense C–O and C=O stretch bands were repeatedly probed with attenuated laser power in order to avoid saturation due to depletion of complexes in the laser beam path.

B. Quantum chemistry calculations

The flexibility of the backbone and carboxyl side arms of the $18c6H_4$ crown demanded a careful exploration of the conformational landscape of the $18c6H_4$–NH_4^+ complex. Simulated annealing was employed to generate an ensemble of molecular structures. The resulting ca. 40 conformations of lowest energy were optimized with density functional theory at the B3LYP/6-31G(d,p) level. Finally, the 15 most stable conformers, spanning free energies within ca. 40 kJ mol^{-1}, were reoptimized with the larger basis set 6-311++G(2d,2p).

The calculations were carried out with the GAUSSIAN 09 code.[24] All energies reported here for the conformers are free energies calculated as the sum of electronic energies plus vibrational zero-point energies and thermal corrections. Nevertheless, the consideration of the uncorrected electronic energies actually led to similar energy differences between the conformers relevant to the present study. The theoretical harmonic IR spectra were calculated by convoluting the normal modes of vibration of the optimized conformers at the B3LYP/6-311++G(2d,2p) level with a line broadening of 15 cm^{-1} (full width at half maximum). The computed vibrational frequencies for all the complexes were scaled for comparison with experiment by a factor 0.975. This factor is in line with the scaling recommended in previous studies for this level of theory,[25, 26] but it is slightly higher than the NIST recommendation.[27]

III. RESULTS

The computational survey of the conformational landscape of the $18c6H_4$–NH_4^+ complex led to the prototypical low energy conformers depicted in Figs. 2 and 3. The most stable conformer 1 displays a barrel–like structure of C_2 symmetry, featuring a tight tetrapodal coordination of ammonium. Such coordination involves two carboxyl groups (C=O$\cdots$HN distance of 1.9 Å), whereas each of the remaining ends of the ammonium cation coordinates in a partly bifurcated way with two consecutive oxygen atoms of the ether ring (O$\cdots$HN distances of 2.1 and 2.4 Å). Such bifurcated arrangement is in contrast with the linear O$\cdots$HN binding found in the complex of NH_4^+ with the native 18–crown–6 ether. The non–bonded carboxyl groups are relatively free to rotate leading to related stationary structures within a few kJ mol^{-1}, such
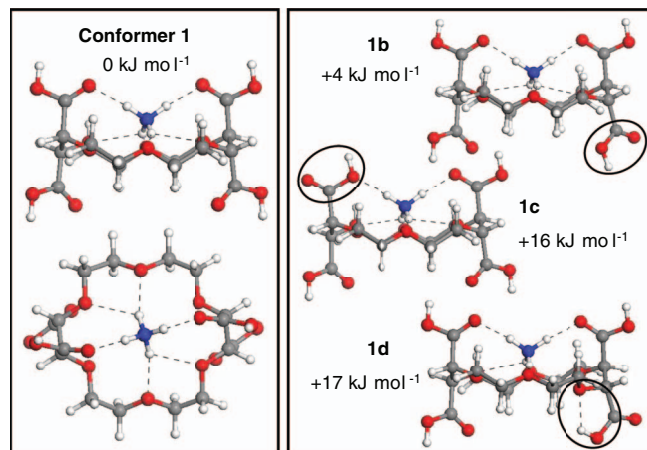
FIG. 2. Representation of the barrel–like most stable conformer 1 of the gas–phase complex $18c6H_4$–NH_4^+ within the B3LYP/6-311++G(2d,2p) computational level. Some low energy variants are also shown (conformers 1b, 1c, and 1d). The most relevant changes with respect to conformer 1 and their corresponding relative free energies are indicated. Conformer 1 is similar to the analogous structure postulated in crystallographic experiments.[13] The rotation of the non–bonded carboxyl groups, e.g. leading to conformer 1b, involves relatively small energy changes. The rotation of one carboxyl group bonded to NH_4^+ (conformer 1c) is endoergic by as much as 16 kJ mol^{-1}. The inversion of the COH angle in conformer 1b to bind the carboxyl group to the ether ring (conformer 1d) involves a similarly high amount of energy.
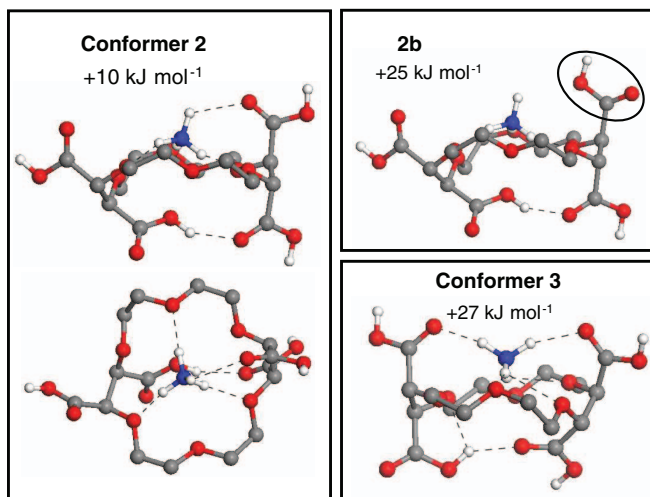
FIG. 3. Representation of the lowest energy bowl–like conformers of the gas–phase complex $18c6H_4$–NH_4^+ within the B3LYP/6-311++G(2d,2p) computational level. The hydrogen atoms of the ether ring are not shown for clarity. The free energy of each conformer relative to the most stable conformer 1 (see Fig. 2) are indicated. The rotation of the carboxyl group leading to conformer 2b reduces the coordination with the ammonium cation and results in a significant increase in energy. Conformer 3 combines features of conformers 1 and 2 and displays a particularly large number of H bonds, although at the cost of a substantial deformation of the substrate backbone and an unfavourable COH angle inversion.

as conformer 1b shown in Fig. 2. In contrast, the rotation of one H−bonded carboxyl to replace the C=O· · ·HN bond with a CHO· · ·HN bond involves a significant increase of energy (e.g., 16 kJ mol^{-1} for conformer 1c). Needless to say that the additional rotation of the second bonded carboxyl (not shown) leads to an increase in energy of similar magnitude. Conformer 1d illustrates that the inversion of the COH angle with respect to conformer 1b is also highly endoergic, in spite of leading to a (in principle) favourable H–bonding interaction of the carboxyl group. It is worth noticing that the prototypical barrel structure is favoured by a low degree of distortion of the ether ring, which maintains a quasiplanar structure.

Figure 3 depicts the most stable bowl–like conformations found in our survey. These conformers are sustained by H–bonding between confronted carboxyl arms (C=O· · ·HO distance of ca. 1.9 Å). In conformer 2 (10 kJ mol^{-1} higher in energy than conformer 1), the ammonium cation rests on top of the ether ring adopting a tripodal coordination (O· · ·HN distances of 1.9–2.0 Å) qualitatively similar to the one found in the ammonium complex with the native 18c6 molecule.[29] The remaining NH coordinates with a C=O group (C=O· · ·HN distance of 2.4 Å). This latter coordination relaxes significantly if the carboxyl group is rotated to expose the COH end instead of the C=O (conformer 2b), leading to an increase of energy of ca. 15 kJ mol^{-1}.

Conformer 3, also shown in Fig. 3, constitutes the next higher prototypical conformation of the complex. It combines features of conformers 1 and 2 to build a particularly large network of H bonds (as many as eight intra- and intermolecular H bonds with O· · ·H distances within 1.9–2.5 Å). However, this occurs in association with a substantial deformation of the $18c6H_4$ backbone and with an unfavourable COH an-

gle inversion. As a consequence, this conformer has a free energy of 27 kJ mol^{-1} above conformer 1. This finding illustrates that the extensive intramolecular bonding allowed by the flexibility of the ether ring and the four carboxyl arms of the $18c6H_4$ molecule is not necessarily favoured in the $18c6H_4$–NH_4^+ complex. It is shown below that the IR spectrum of this conformer is not consistent with the experimental IRMPD spectrum recorded for the complex, meaning that its population is negligible under the present working conditions.

A broad ensemble of higher energy barrel–like and bowl–like conformers with different degrees of H–bonding were found in the computational survey. Those conformers, all lying higher than 28 kJ mol^{-1} above conformer 1 within the B3LYP/6-311++G(2d,2p) level of theory, are unlikely to contribute to the present experiment and will not be considered for the present discussion.

The experimental IRMPD spectrum of the $18c6H_4$–NH_4^+ complex is shown in Fig. 4. The corresponding harmonic IR absorption spectra predicted by the B3LYP computation for the conformers 1, 2, 1c, 1d, and 3, described in the preceding paragraphs and in Figs. 2 and 3, are also shown for direct comparison. For the sake of discussion, the different vibrational bands observed in the experimental spectrum are labelled A through J in order of increasing wavenumber. The dominant type of nuclear motion of the vibrational modes associated with each of the bands is described in Table I. Bands A, B, C, and J arise from vibrational modes driven by the carboxyl arms, namely, torsion of the OH bond out of the COOH plane (band A), bending of the OCO bond angle (band B), a peculiar umbrella–type vibration of the CCOO moiety with the carboxyl carbon as vibrational center (band C), and the stretching modes of the bonded and non-bonded C=O groups (band J). Bands D (C–C stretching), E (C–O stretching), and F and H (CH_2 deformation modes) correspond to typical vibrational motions of the crown ether ring also observed in the cation complexes of the native 18c6 molecule.[25,28,29] Band G (and partly also band E) are associated to wagging or torsional motions of the HCCH sequence linked to the side carboxyl arms. Finally, band I is dominated by wagging of NH_4^+, strongly coupled to scissoring vibration of the CH_2 groups of the ether ring.

A broad band, not fully predicted by the B3LYP calculations, is neatly appreciated in the IRMPD spectra at around 1425 cm^{-1} (band labelled with an asterisk in Fig. 4). Noticeably, a similar unpredicted band was also observed within this wavenumber region in the complexes of NH_4^+ with the unsubstituted crown ethers 15c5 and 18c6,[29] as well as in protonated ammonia clusters.[30,31] Hence, this spectral feature seems to be intrinsic to ammonium in non-covalent complexes. The assignment of the band to ammonium vibrations was corroborated by measurements with the isotopic variant ND_4^+.[29] For the protonated ammonia clusters, this band could be ascribed from quantum calculations to a combination band of symmetric and antisymmetric stretching modes.[30,31] Similar calculations for the present complexes are challenging and well beyond the scope of this study, and it is thus not straightforward to confirm such assignment.

According to the results of the B3LYP/6-311++G (2d,2p) computations outlined above, the barrel–like
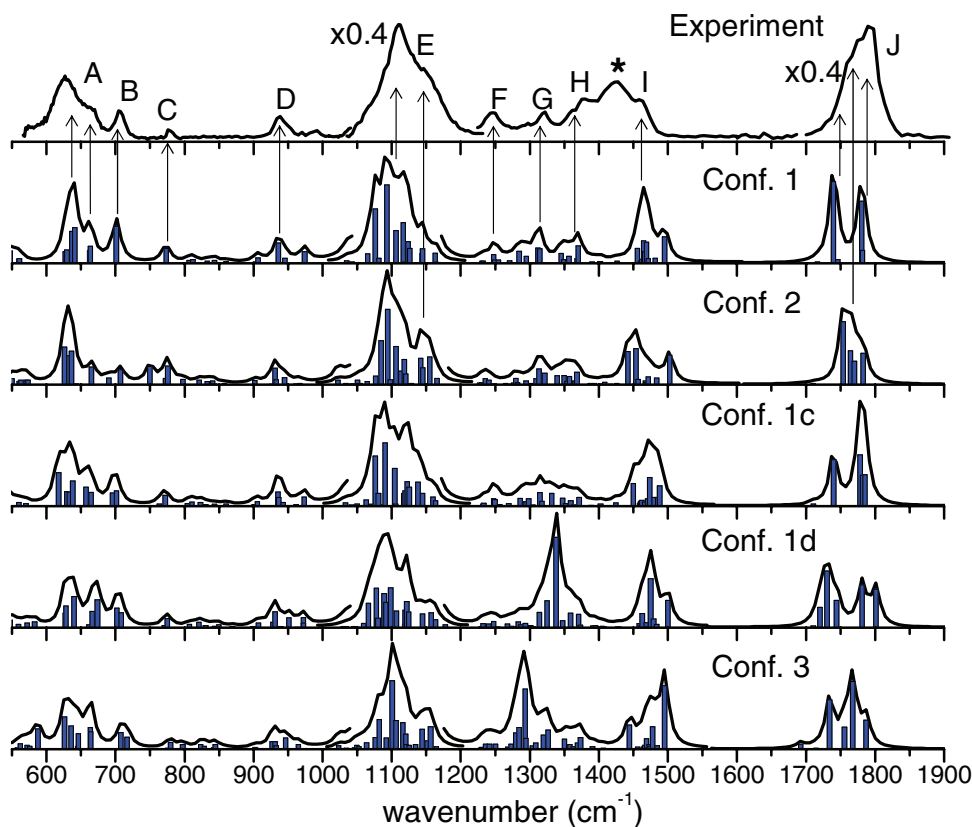
FIG. 4. ESI–FT–ICR IRMPD spectrum of the gas–phase (18c6H$_4$)–NH$_4^+$ complex (top panel). The corresponding harmonic IR spectra predicted by the B3LYP/6-311++G(2d,2p) computation for relevant low energy conformers depicted in Figs. 2 and 3 are also shown for direct comparison. The intensities of all the spectra in the regions of the intense C–O and C=O stretching bands (1000–1200 cm^{-1}, and 1700–1900 cm^{-1}, respectively) have been rescaled by a factor of 0.4 for a better visualization of the weaker bands. The vibrational bands observed in the experimental spectrum are labelled A through J in order of increasing wavenumber, and the dominant types of nuclear motions of the corresponding vibrational modes are described in Table I.

conformer 1 and the bowl–like conformer 2 should dominate the conformational behavior of the 18c6H$_4$–NH$_4^+$ complex at the room temperature of the present experiments. Figure 4 corroborates such expectation by showing

TABLE I. Vibrational mode assignment based on the B3LYP/6-311++G(2d,2p) calculation for the main bands observed in the IRMPD spectra of this work. The dominant type of vibration (in boldface) and significant secondary types of vibration are indicated in each case. Bands are labelled A through J, in order of increasing wavenumber.

Band	Mode assignment
A	**OCOH torsion**; COC bending
B	**Carboxyl OCO bending**; OCOH torsion
C	**Umbrella CCOO vibration** (carboxyl arms)
D	**C–C stretching**; CH$_2$ rocking
E	**C–O–C stretching**; COH bending, CH$_2$ rocking, torsion of HCCH[a]
F	**CH$_2$ twisting**; COH bending
G	**CH wagging**[a]; COH bending
H	**CH$_2$ wagging**; COH bending
I	**NH$_4^+$ wagging**, CH$_2$ scissoring
J	**C=O stretching**
*	**NH$_4^+$ stretching (combination band)** (tentative from Refs. 30 and 31)

[a]In carbons attached to carboxyl arms.

an excellent matching between the experimental IRMPD spectrum and the joint contribution of the computational IR bands of conformers 1 and 2. The low energy variants of these two conformers that result from the rotation of the free carboxyl groups, e.g. conformer 1b, should also be populated in the experiment. However, the changes induced by such rotation in the IR spectra are negligible within the resolution of the laser system employed, so that their likely contribution to the experimental IRMPD signal is enclosed within the one assigned here to conformers 1 and 2.

The computed spectrum for conformer 1 reproduces accurately the main features of the experimental vibrational bands, in particular, the detailed structure of the weaker bands in the ranges 550–1000 cm^{-1} (bands A–D) and 1200–1550 cm^{-1} (bands F–I). On the other hand, the fine details of the envelopes of the C–O and C=O stretching bands (bands E and J, respectively) are somewhat less accurately described by the computation. The B3LYP spectrum of conformer 1 seems to underestimate the intensity of the blue shoulder of band E at 1150–1200 cm^{-1}. Furthermore, conformer 1 displays a C=O stretching band of bimodal shape due to the two differentiated pairs of bonded and free carboxyl groups. In contrast, the IRMPD spectrum displays a broad band within 1725–1850 cm^{-1} with a hint for oscillations which is compatible with the bimodal band structure

but suggests the contribution of additional C=O stretching components. It can be appreciated in Fig. 4 that the incorporation of conformer 2 to the analysis solves these latter discrepancies and brings the computation to virtual full accord with the experiment. On one hand, band E of conformer 2 displays a structured envelop that serves to reproduce the blue shoulder and also the relatively sharp maximum of the experimental band around 1120 cm^{-1}. Furthermore, the merging of the C=O stretching components in conformer 2, added up to the bimodal band of conformer 1, explains the broad band structure observed experimentally.

The precise relative populations of conformers 1 and 2 in the experiment are difficult to determine from the IRMPD spectrum. Nevertheless, a contribution from conformer 2 to the IRMPD intensity of not less than about 30% is required in order to reproduce the observed bands E and J from the computed spectra. Such a significant value suggests that, if thermodynamical equilibrium among the conformers is assumed, the relative energy of 10 kJ mol^{-1} predicted for conformer 2 may be significantly overestimated by the B3LYP computation. Alternatively, the interconversion barriers between conformer 2 and conformer 1 might be sufficiently high as to induce kinetic trapping of the higher energy conformer 2 under the present experimental conditions.[13] This would result in a non–equilibrium distribution favouring a population of conformer 2 higher than expected from energetics.

Conformers 1c and 1d are unlikely to be populated in the experiment, in view of their comparably high energies with respect to conformer 1. In fact, whereas the B3LYP IR spectra of these conformers display some common features with the measured IRMPD spectrum, appreciable differences are also apparent which rule out any significant contribution to the recorded signal. Spectral features particularly in contrast with experiment are found in the spectra computed for these conformers in the 1200–1500 cm^{-1} range. Conformer 1d displays a strong band at 1340 cm^{-1}, not present in the IRMPD spectrum, that is directly associated with a bending vibration in the COH group H-bonded to the ether ring (see Fig. 2). The differences with the IRMPD measurement for conformer 1c are more subtle and mainly related to the lack of structure in the computed spectrum at 1200–1500 cm^{-1} due to the spread of the many COH bending and the CH$_2$ deformation modes.

Figure 4 also serves to corroborate that conformer 3 cannot have an appreciable population under the present experimental conditions, in spite of its extensive H–bonding network. The B3LYP IR spectrum of conformer 3 displays two strong bands at around 1290 cm^{-1} and 1500 cm^{-1} for which no trace is found in the IRMPD spectrum. According to the B3LYP computation, the 1290 cm^{-1} band is related to CH wagging and bending of the COH group participating in the carboxyl–carboxyl H bond (hence, it is analogous to band G in conformer 1), whereas the 1500 cm^{-1} band of this conformer is dominated by an umbrella motion of the NH$_4^+$ guest.

We close the discussion by bringing the present benchmark gas–phase study into relation with previous investigations of the title system in condensed phases. First of all, it is worth noticing that conformer 1 described here for the 18c6H$_4$–NH$_4^+$ complex is remarkably close to the structure derived from x–ray crystallographic measurements in a previous work.[13] This is an interesting finding since in our study the 18c6H$_4$ host is in the neutral charge state, whereas in the crystallographic study it was in the monoanionic 18c6H$_3^-$ form. Deprotonation of one or more carboxyl groups of 18c6H$_4$ can actually be expected to reinforce the barrel–like conformations due to the ionic character of the carboxylate–ammonium interactions. This aspect plausibly contributes to the concordance between the gas–phase and the crystallographic studies found here. Also interestingly, the non–bonded carboxyl groups were found to be bridged by one water molecule in the crystalline arrangement, which suggests facile hydration of this conformation without significant structural changes. Second of all, the bowl–like structure of the present conformer 2 is similar to the one typically postulated to be responsible for the chiral separation of racemic secondary amines in solution.[13] The stabilization of the bowl–like conformation requires that at least one of the carboxylate moieties remains protonated, which demands an acidic environment (pH values smaller than ∼5).[32] Otherwise, the barrel–like arrangements would dominate the conformational landscape of the complex.

IV. SUMMARY AND CONCLUDING REMARKS

A combined spectroscopic and computational study has been performed in order to gain insights into the conformational features of the 18c6H$_4$–NH$_4^+$ complex, formed by a benchmark tetracarboxyl crown ether with the ammonium cation.

The most stable conformation postulated by the computation for the isolated complex (conformer 1) corresponds to a barrel–like arrangement of C_2 symmetry and a quasiplanar ether ring that is essentially coincident with the structure determined in crystallographic studies. Such conformation involves a tetrapodal coordination of the NH$_4^+$ cation with two C=O groups from confronted carboxyl side arms and with four oxygen atoms of the ether ring in a partially bifurcated arrangement.

The next prototypical conformation in terms of energy (conformer 2) is a bowl–like structure characterized by the H–bonding between two carboxyl groups on opposite sides of the ring. The NH$_4^+$ cation also displays a tetrapodal coordination with the crown ether, in this case with three oxygen atoms of the ether ring and with one C=O group of a carboxyl arm. This conformation is closely related to the analogous bowl–like structures adopted by 18c6H$_4$ when binding secondary amines.

The joint contribution of the IR absorbances predicted by the B3LYP/6-311++G(2d,2p) computation for conformers 1 and 2 (including their low energy variants associated with the facile rotation of the non-bonded carboxylic groups) provides an excellent matching of the experimental action spectrum measured with the IRMPD technique. It can be therefore concluded that these barrel–like and bowl–like structures define the conformational behavior of the gas–phase 18c6H$_4$–NH$_4^+$ complex at room temperature. Complementary IR spectroscopy studies of the title system, covering the O–H stretching range, would be very valuable to obtain a more

accurate estimation of the relative contribution of the two types of conformations.

The close relation found between the conformational features of the $18c6H_4$–NH_4^+ complex in the gas phase and those found in the previous crystalline (x–ray) and solution (NMR) studies is particularly interesting. This was not necessarily expected due to the different deprotonated forms and the appreciable flexibility of the $18c6H_4$ substrate, leading to a variety of potential arrangements to bind the NH_4^+ cation. It appears that the barrel–like and the bowl–like arrangements are optimal for the commensurate multipodal binding with ammonium (and protonated amines). The relative stability of these two types of conformations may be subtle, especially when effects due to solvation and partial deprotonation of the host are incorporated. Moreover, transitions between the two conformations may take place depending on the type of coordination with the guest cation, as demonstrated by the x–ray investigations on crystalline networks.[13] Nevertheless, it has been gratifying to find that the general features of the barrel and bowl arrangements, in particular, the intramolecular and intermolecular coordination constraints that drive the complexation of $18c6H_4$ with molecular cations, can be investigated in the isolated state. This approach provides a direct link between the experimental data and the computational techniques, since the molecular system is prepared under well–defined environmental conditions. The present study has served to validate the comparably inexpensive B3LYP/6-311++G(2d,2p) computational framework for the description of the molecular architecture of the title system. Whereas the relative energy difference between the barrel– and bowl–like structures appears to be overestimated by several kJ mol^{-1} by this level of computation, a definite assessment to this respect would require a more involved investigation of kinetic trapping effects, plausibly leading to non–equilibrium populations for the low energy conformers of the title complex.

[1] S. Kobayashi, T. Hamada, S. Nagayama, and K. Manabe, J. Braz. Chem. Soc. **12**, 627–633 (2001).

[2] L. Yang, L. D. Tang, Y. M. Pan, H. S. Wang, G. F. Su, and M. Liang, Chin. J. Org. Chem. **28**, 1250–1253 (2008).

[3] Y. Kuwahara, H. Nagata, H. Nishi, Y. Tanaka, and K. Kakehi, Chromatographia **62**, 505–510 (2005).

[4] H. Nishi, K. Nakamura, H. Nakai, and T. Sato, J. Chromatogr. A **757**, 225–235 (1997).

[5] R. Kuhn, Electrophoresis **20**, 2605–2613 (1999).

[6] T. Lee, W. Lee, M. H. Hyun, and J. H. Park, J. Chromatogr. A **1217**, 1425–1428 (2010).

[7] M. Lammerhofer, J. Chromatogr. A **1217**, 814–856 (2010).

[8] M. H. Hyun, J. Sep. Sci. **29**, 750–761 (2006).

[9] Y. Machida, H. Nishi, and K. Nakamura, J. Chromatogr. A **810**, 33–41 (1998).

[10] Y. Machida, M. Kagawa, and H. Nishi, J. Pharm. Biomed. Anal. **30**, 1929–1942 (2003).

[11] A. E. Lovely and T. J. Wenzel, Chirality **20**, 370–378 (2008).

[12] P. Gerbaux, J. de Winter, D. Cornil, K. Ravicini, G. Pesesse, J. Cornil, and R. Flammang, Chem.-Eur. J. **14**, 11039–11049 (2008).

[13] H. Nagata, H. Nishi, M. Kamigauchi, and T. Ishida, Chirality **20**, 820–827 (2008).

[14] H. Nagata, H. Nishi, M. Kamigauchi, and T. Ishida, Chem. Pharm. Bull. (Tokyo) **54**, 452–457 (2006).

[15] H. Nagata, Y. Machida, H. Nishi, M. Kamigauchi, K. Minoura, and T. Ishida, Bull. Chem. Soc. Jpn. **82**, 219–229 (2009).

[16] E. Bang, J.-W. Jung, W. Lee, D. W. Lee, and W. Lee, J. Chem. Soc., Perkin Trans. **2**, 1685–1692 (2001).

[17] J.-P. Schermann, *Spectroscopy and Modelling of Biomolecular Building Blocks* (Elsevier, Amsterdam, 2008).

[18] J. P. Simons, Mol. Phys. **107**, 2435–2458 (2009).

[19] M. S. de Vries and P. Hobza, Annu. Rev. Phys. Chem. **58**, 585–612 (2007).

[20] N. C. Polfer and J. Oomens, Mass Spectrom. Rev. **28**, 468–494 (2009).

[21] T. R. Rizzo, J. A. Stearns, and O. V. Boyarkin, Int. Rev. Phys. Chem. **28**, 481–515 (2009).

[22] See http://www.rijnh.nl/felix/ for information about the free-electron laser facility.

[23] N. C. Polfer and J. Oomens, Phys. Chem. Chem. Phys. **9**, 3804–3817 (2007).

[24] M. J. Frisch, G. W. Trucks, H. B. Schlegel *et al.*, GAUSSIAN 09, Revision A.1, Gaussian, Inc., Wallingford, CT, 2009.

[25] F. Gamez, P. Hurtado, B. Martínez–Haya, G. Berden, and J. Oomens, Int. J. Mass Spectrom. **308**, 217–224 (2011).

[26] S. Z. Fairchild, C. F. Bradshaw, S. U. Wangsheng, and S. K. Guharay, Appl. Spectrosc. **63**, 733–741 (2009).

[27] NIST Standard Reference Database 101; Computational Chemistry Comparison and Benchmark DataBase; see http://cccbdb.nist.gov/vibscalejust.asp.

[28] B. Martínez-Haya, P. Hurtado, A. R. Hortal, S. Hamad, J. D. Steill, and J. Oomens, J. Phys. Chem. A **114**, 7048–7054 (2010).

[29] P. Hurtado, F. Gámez, S. Hamad, B. Martínez-Haya, J. D. Steill, and J. Oomens, J. Phys. Chem. A **115**, 7275–7282 (2011).

[30] K. R. Asmis, Y. Yang, G. Santambrogio, M. Brümmer, L. R. McCunn, J. R. Roscioli, M. Johnson, O. Kühn, and D. J. Goebbert, Angew. Chem., Int. Ed. **46**, 8691–8694 (2007).

[31] Y. Yang, O. Kühn, G. Santambrogio, D. J. Goebbert, and K. R. Asmis, J. Chem. Phys. **129**, 224302 1-8 (2008).

[32] P. J. Dutton, T. M. Fyles, and S. J. McDermid, Can. J. Chem. **66**, 1097–1108 (1988).